

© 2018. The American Astronomical Society. All rights reserved. Access to this work was provided by the University of Maryland, Baltimore County (UMBC) ScholarWorks@UMBC digital repository on the Maryland Shared Open Access (MD-SOAR) platform.

Please provide feedback

Please support the ScholarWorks@UMBC repository by emailing scholarworks-group@umbc.edu and telling us

what having access to this work means to you and why it's important to you. Thank you.

BLAZAR SHEATH ILLUMINATION OF THE OUTER MOLECULAR TORUS: A RESOLUTION OF THE SEED PHOTON PROBLEM FOR THE FAR-GEV BLAZAR FLARES

PETER BREIDING,¹ MARKOS GEORGANOPOULOS,^{1,2} AND EILEEN T. MEYER¹

¹*Department of Physics, University of Maryland Baltimore County, Baltimore, MD 21250, USA*

²*NASA Goddard Space Flight Center, Code 660, Greenbelt, MD 20771, USA*

ABSTRACT

Recent multiwavelength work led by the Boston University blazar group (e.g., [Marscher et al. 2010](#)) strongly suggests that a fraction of the blazar flares seen by the *Fermi* Large Area Telescope (LAT) take place a few to several pc away from the central engine. However, at such distances from the central engine, there is no adequate external photon field to provide the seed photons required for producing the observed GeV emission under leptonic inverse Compton (IC) models. A possible solution is a spine-sheath geometry for the emitting region ([MacDonald et al. 2015](#), but see [Nalewajko et al. 2014](#)). Here we use the current view of the molecular torus (e.g., [Elitzur, 2012](#); [Netzer 2015](#)) in which the torus extends a few pc beyond the dust sublimation radius with dust clouds distributed with a declining density for decreasing polar angle. We show that for a spine-sheath blazar jet embedded in the torus, the wide beaming pattern of the synchrotron radiation of the relatively slow sheath will heat molecular clouds whose subsequent IR radiation will be seen highly boosted in the spine comoving frame, and that under reasonable conditions this photon field can dominate over the sheath photons directly entering the spine. If the sheath is sufficiently luminous it will sublimate the dust, and if the sheath synchrotron radiation extends to optical-UV energies (as may happen during flares), this will illuminate the sublimated dust clouds to produce emission lines that will vary in unison with the optical-UV continuum, as has been very recently reported for blazar CTA 102 ([Jorstad et al. 2017](#)).

Keywords: galaxies: active—quasars: general—radiation mechanisms: non-thermal—
gamma rays: galaxies

1. INTRODUCTION

Blazars, radio loud active galactic nuclei (AGN) with their relativistic jets pointed at small angles to the line of sight (Blandford & Rees 1978), exhibit powerful flares of gamma-ray emission (e.g. Abdo et al. 2010). In the context of leptonic models, the gamma-ray emission of powerful blazars is considered to be due to inverse Compton (IC) scattering of low-energy seed photons from the sub-pc size broad-line region (BLR; Sikora et al. 1994) and/or the pc-scale molecular torus (MT, Błażejowski et al. 2000). These seed photons are in turn produced when the semi-isotropically emitting accretion disk illuminates the BLR and MT.

A related seed photon production mechanism that motivated this work is the illumination of BLR clouds by the beamed optical-UV radiation of the blazar itself (Ghisellini & Madau 1996). Because the blazar emission is beamed within a small angle ($\sim 1/\Gamma \lesssim 5^\circ$), where $\Gamma \gtrsim 10$ is the bulk Lorentz factor of the flow), this model requires the existence of BLR clouds within this very small polar beaming angle.

The above mechanisms posit that the GeV emitting region is within a pc or less from the central engine. However, multiwavelength monitoring (e.g. Marscher et al. 2010), including VLBI imaging, reveals that at least a fraction of flares occur at the location of the VLBI core. The inference that some gamma-ray flares originate near the location of the VLBI core results from the strong correlations seen in light curves from radio through gamma-ray wavelengths during these flares, and the fact that often a superluminal component is seen ejected from the VLBI core near the peak time of the GeV flare: in PKS 1510-089, one of the most well documented cases (Marscher et al. 2010), a radio and optical flare takes place at the same time with a GeV flare and a new component emerges from the VLBI core. The core may be the site of a standing shock few to several pc downstream of the central engine. Alternatively, it can be the location where the jet at the frequency of observation becomes optically thick, again few to several pc downstream of the central engine. One can discriminate between these two possibilities, as in the first case the location of the core does not change with the frequency of VLBI observation, while in the second it shifts closer to the central engine as the frequency of observation increases (e.g., Hada et al. 2011).

The far GeV flares show that powerful blazar jets produce gamma-ray emission beyond the canonical sub-pc scale BLR and pc-scale MT. At such large distances, however, there is no substantial source of seed photons for the IC process from the BLR or the MT, as both photon fields illuminate the blazar from behind and are therefore substantially de-beamed in the comoving frame of the emitting plasma (Dermer et al. 1992; Nalewajko et al. 2014). An alternative source of seed photons arises if we consider that the jet is characterized by a fast spine in which the plasma flows with a Lorentz factor of the order of $\Gamma_{sp} \sim 10 - 20$, surrounded by a slow sheath through which the plasma flows with a Lorentz factor of the order of $\Gamma_{sh} \sim \text{few}$ (Ghisellini et al. 2005). In this case the energy density of the sheath photons will be seen to be Doppler boosted in the spine comoving frame by $\sim \Gamma_{sp}^2/(4\Gamma_{sh}^2)$ (Nalewajko et al. 2014). MacDonald et al. (2015) applied the spine-sheath model to the blazar PKS 1510-089 and showed that with a judicious choice of model parameters it can reproduce the observed variability. However, Nalewajko et al. (2014) argued that the spine-sheath boosting is inadequate for producing the required seed photon energy density in the frame of the spine without requiring a sheath spectral energy distribution (SED) that overproduces the observed blazar SED.

Our current view of the MT suggests another source of seed photons. Originally, the AGN unification scheme (e.g. Antonucci 1993) suggested that the dichotomy between type 1 and type 2 AGN

spectra can be explained as an orientation effect due to an opaque equatorial MT. More recent observational and theoretical work (e.g. [Nenkova et al. 2008](#); [Elitzur, 2012](#); [Netzer 2015](#)) support the idea that the MT is clumpy ([Krolik & Begelman 1988](#)) and, furthermore, that the distribution of the dusty clumps is a gradually declining function of decreasing polar angle, allowing for some fraction of dusty clumps to lie at relatively small polar angles (e.g., [García-González et al. 2017](#); [Khim & Yi 2017](#)). The inner radius R_d of the MT is set by dust sublimation due to the radiation of the accretion disk and has been measured by near-IR interferometry (e.g., [Kishimoto et al. 2011](#)) and near IR reverberation mapping (e.g., [Koshida et al. 2014](#)) of nearby Seyferts to have a size that for bright AGN (accretion disk luminosity $L_{\text{optical-UV}} \sim 10^{46} \text{ erg s}^{-1}$) would be $R_d \sim 1 \text{ pc}$ ([Nenkova et al. 2008](#)).

The BLR is contained within the dust sublimation radius R_d . The outer radius of the MT is found both with modeling the MT SED ([Fuller et al. 2016](#)) and through Atacama Large Millimeter/sub-millimeter array (ALMA) observations ([García-Burillo et al. 2016](#); [Gallimore et al. 2016](#)) to be of the order of a few to several pc, several times larger than R_d , with most of the MT power emitted in the IR from the clouds at $\sim R_d$ ([Nenkova et al. 2008](#)). With this configuration it is plausible that the blazar radio core, identified with the blazar GeV flaring site (e.g. [Marscher et al. 2010](#)) is located beyond R_d but within the outer bounds of the MT.

Here we show that in the context of a spine-sheath configuration, a moderately relativistic sheath located within the MT beyond R_d can illuminate a substantial solid angle of the clumpy dusty material that lies beyond it, out to the outer bounds of the MT. In §2 we show that the radiation of these illuminated clumps, seen in the frame of the fast spine, can dominate over the sheath radiation in the spine co-moving frame and act as the required external photon field. In §3 we present a general model SEDs using a motivated set of model parameters, and in §4 we present our conclusions and discuss some of the implications of our model.

2. THE PHOTON ENERGY DENSITY IN THE JET SPINE

Our picture (figure 1) for the far GeV blazar emission posits a standing jet feature, possibly a recollimation shock, a few to several pc from the black hole. Plasma flows through the standing feature, which has a spine bulk Lorentz factor $\Gamma_{sp} \sim 10 - 20$ and a slower outer sheath with bulk Lorentz factor $\Gamma_{sh} \sim 2 - 4$. To keep the study analytically tractable we approximately assume $1 \ll \Gamma_{sh} \ll \Gamma_{sp}$. Dusty molecular clouds within the wide (up to $\theta_{sh} \sim 1/\Gamma_{sh} \lesssim 30^\circ$) beaming angle of the synchrotron-emitting sheath reprocess a fraction of this radiation, which is then relativistically amplified in the fast spine rest frame. The observed GeV emission is attributed to IC scattering of these photons by the relativistic electrons in the fast spine, provided this photon energy density dominates over that of the sheath photon field directly entering the spine.

We assume that the sheath produces an isotropic synchrotron luminosity L'_{sh} in its comoving frame, peaking in the sub-mm to IR, as the synchrotron SEDs of powerful blazar usually do (e.g. [Meyer et al. 2011](#)). In the galaxy frame, the solid-angle integrated luminosity (the luminosity that a hypothetical detector covering all 4π of the sky of the source would measure) is $L_{sh} = \Gamma_{sh} L'_{sh}$, valid assuming that the sheath is a stationary feature. Most of this radiation is beamed into a solid angle $\Omega_{sh} = \pi/\Gamma_{sh}^2$ (opening half-angle $\sim 1/\Gamma_{sh}$) and for simplicity we assume that within this angle the intensity of the radiation does not vary. An observer within this solid angle that assumes that the source is isotropic

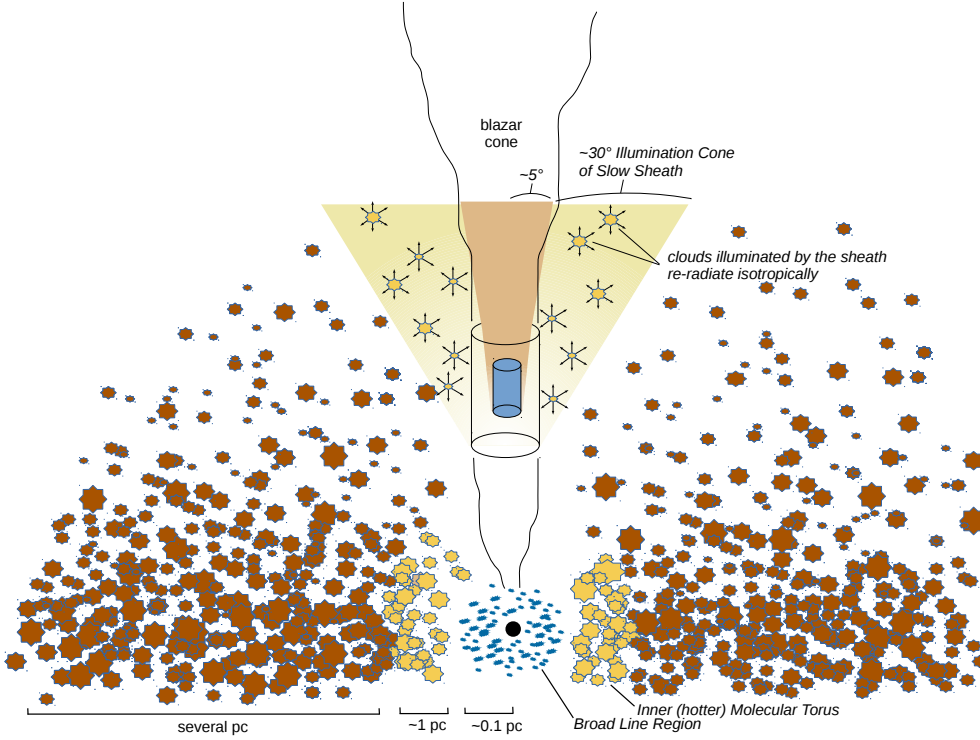


Figure 1. A schematic representation of the spine-sheath blazar embedded in the MT (not to scale). The MT is clumpy and the clouds have a number density that declines with decreasing polar angle. The blazar site is far beyond its traditional location within the BLR and/or the inner, hotter part of the MT: it is at a distance of a few pc but still within the MT. The wide beaming angle of its sheath synchrotron emission illuminates and heats the MT clouds within the Sheath’s synchrotron emission opening angle and these in turn radiate isotropically. This radiation can provide the dominant seed photon field for IC scattering in the spine comoving frame. Note that the spine beaming angle is very small ($\lesssim 5^\circ$) and it is not expected to be intercepted by any MT clouds.

in her/his frame will infer a luminosity

$$L_{sh,obs} = L_{sh} 4\pi / \Omega_{sh} = 4\Gamma_{sh}^2 L_{sh} = 4\Gamma_{sh}^3 L'_{sh}. \quad (1)$$

The sheath synchrotron radiation illuminates MT dust clouds, which for simplicity we assume are isotropically and homogeneously distributed within the solid angle Ω_{sh} , starting from the sheath radius R_{sh} and extending to some distance R_{out} with a sheath covering factor C (where C is the fraction of obscured solid angle within the sheath beaming cone). We treat the dust clouds as ideal spherical black bodies which act as perfect absorbers to the sheath emission. The dust clouds then absorb and are heated by the sheath radiation. Sublimation of the dust occurs for those clouds that are at

distances from the sheath less than their sublimation radius

$$R_{sub} = \left(\frac{L_{sh,obs}}{16\pi\sigma T_{sub}^4} \right)^{1/2}, \quad (2)$$

where T_{sub} is the dust sublimation temperature, and $\sigma = 5.67 \times 10^{-5} \text{ erg cm}^{-2} \text{ deg}^{-4} \text{ s}^{-1}$ is the Stefan-Boltzmann constant. The minimum $L_{sh,obs}$ that can cause sublimation is found by the requirement $R_{sub} = R_{sh}$ and is

$$L_{\star} = 16\pi\sigma T_{sub}^4 R_{sh}^2 = 2.85 \times 10^{45} T_{sub,3}^4 R_{sh,18}^2 \text{ erg s}^{-1}, \quad (3)$$

where $T_{sub,3}$ is the dust sublimation temperature in units of 1000 K, and $R_{sh,18}$ is the sheath radius in units of 10^{18} cm. For $L_{sh,obs} < L_{\star}$ the sheath radiation heats but does not sublimate the dust, while for $L_{sh,obs} > L_{\star}$ the dust is sublimated up to a distance R_{sub} given by equation (2). As we require that the observed blazar SED is dominated by the spine and not by the sheath, and as the typical synchrotron SED for powerful blazars has an observed power of $\sim 10^{46} \text{ erg s}^{-1}$ (e.g. Meyer et al. 2011), we assume here that $L_{sh,obs} < L_{\star}$ (i.e. $\eta \equiv L_{sh,obs}/L_{\star} < 1$) and no sublimation takes place.

2.1. Photon energy density in the spine due to sheath radiation reprocessed by the clouds

We proceed now to derive the intensity of the radiation received back from the dust clouds within Ω_{sh} , and from this the corresponding photon energy density in the co-moving frame of the fast spine. For this we assume that all of the sheath power absorbed by the clouds found at $R_{sh} < R < R_{out}$ and within Ω_{sh} is isotropically re-radiated as thermal black body radiation for the dust clouds.

At a distance r from the center of the spine-sheath system, the sheath power absorbed by a shell of differential width dr is

$$dP_{abs} = \frac{L_{sh}C}{R_{out} - R_{sh}} dr = \frac{L_{sh,obs}\Omega_{sh}C}{4\pi(R_{out} - R_{sh})} dr. \quad (4)$$

This power is then re-radiated by each shell with an emissivity given by:

$$\epsilon = \frac{dP_{abs}}{dV} = \frac{dP_{abs}}{\Omega_{sh}r^2 dr} = \frac{L_{sh,obs}C}{(R_{out} - R_{sh})4\pi r^2}. \quad (5)$$

Assuming isotropic emission for each shell, the emission coefficient, J , can be written as $J = \epsilon/4\pi$. The intensity contribution from each infinitesimal shell is then given by $dI(r) = Jdr$, and the total intensity of the radiation field received back from the dust clouds is

$$I = \int_{R_{sh}}^{R_{out}} Jdr = \frac{L_{sh,obs}C}{16\pi^2 R_{out} R_{sh}} = \frac{L_{sh,obs}C}{16\pi^2 a R_{sh}^2}, \quad (6)$$

where $a \equiv R_{out}/R_{sh} > 1$.

The energy density of this radiation field in the host galaxy frame at the location of the spine is $U = (1/c) \int_{\Omega_{sh}} I d\Omega = (1/c) I \Omega_{sh}$ (c is the speed of light), as in our approximate treatment the intensity does not have an angular dependence within Ω_{sh} . Using $\Omega_{sh} = \pi/\Gamma_{sh}^2$ we then obtain:

$$U = \frac{\pi I}{c\Gamma_{sh}^2} = \frac{L_{sh,obs}C}{16\pi a R_{sh}^2 c\Gamma_{sh}^2}. \quad (7)$$

Recalling that $\eta = L_{sh,obs}/L_*$ and using equation (3) allows us to put this equation in the following form:

$$U = \frac{4\sigma T_{sub}^4}{c} \frac{\eta C}{4a\Gamma_{sh}^2}. \quad (8)$$

Note that the first fraction in the above equation is a blackbody energy density and the second fraction is a dimensionless dilution factor. The energy density in the rest frame of the spine flow plasma can be shown to be $U'' = 4U\Gamma_{sp}^2$ (following a calculation similar to [Dermer & Schlickeiser 1994](#)), where double primed variables refer to the co-moving frame of the spine flow:

$$U'' = \frac{L_{sh,obs}C}{4\pi a R_{sh}^2 c} \frac{\Gamma_{sp}^2}{\Gamma_{sh}^2} = \frac{4\sigma T_{sub}^4}{c} \frac{\eta C}{a} \frac{\Gamma_{sp}^2}{\Gamma_{sh}^2} \quad (9)$$

2.2. Photon energy density in the spine coming directly from the sheath

Assuming isotropic emission in the rest frame of the sheath, the energy density of the sheath's synchrotron radiation in its comoving frame is given by:

$$U'_{sh} = \frac{L'_{sh}}{4\pi R_{sh}^2 c} = \frac{L_{sh,obs}}{16\pi R_{sh}^2 c \Gamma_{sh}^3}, \quad (10)$$

where we have used eq. (1). The energy density of this photon field in the spine frame is $U''_{sh} = (4/3)U'_{sh}\Gamma_{rel}^2$ ([Dermer & Schlickeiser 1994](#)), where Γ_{rel} is the relative Lorentz factor between the spine and the sheath, given by $\Gamma_{rel} = \Gamma_{sh}\Gamma_{sp}(1 - \beta_{sh}\beta_{sp}) \approx \Gamma_{sp}/(2\Gamma_{sh})$. Using these we can write:

$$U''_{sh} = \frac{L_{sh,obs}\Gamma_{sp}^2}{48\pi R_{sh}^2 c \Gamma_{sh}^5} = \frac{4\sigma T_{sub}^4}{c} \eta \frac{\Gamma_{sp}^2}{12\Gamma_{sh}^5}, \quad (11)$$

where we have used equation (3).

2.3. Comparison of the energy densities in the spine

The ratio of the energy density in the spine rest frame due to the photon field received in the spine from the illuminated MT clouds to the photon field directly illuminating the spine by the sheath is

$$\frac{U''}{U''_{sh}} = \frac{12C\Gamma_{sh}^3}{a}. \quad (12)$$

In the case of a low but non-negligible covering factor, as is plausible in this setting (see §4), we can set $12C = 1$. Also, the sheath is constrained to be substantially slower than the $\Gamma_{sp} \sim 10 - 20$ spine, and still be relativistic, as otherwise we would detect the counter-sheath with VLBI observations. A plausible value for the sheath Lorentz factor is $\Gamma_{sh} = 3$. For these values of C and Γ_{sh} the condition for the cloud-reprocessed radiation energy density in the spine to be comparable to or dominate over that coming directly from the sheath becomes $a = R_{out}/R_{sh} \lesssim 27$. For example, adopting and setting $R_{sh} = 0.2$ pc ([MacDonald et al. 2015](#)), we see that the cloud processed photon energy density dominates if the sheath-spine system is embedded in the MT by less than $\sim 10 R_{sh} \sim 2$ pc. In the framework where some GeV flares come from distances of a few pc and the clumpy MT extending for a few pc this condition is plausible.

2.4. Viability of SSC for powerful blazars

We now address whether the GeV emission of powerful blazars can be synchrotron-self Compton (SSC, e.g. [Maraschi et al. 1992](#)) emission. To evaluate this, we approximate the emission region with a sphere of radius R , permeated by a magnetic field B , and moving relativistically with Doppler factor δ relative to the observer. Electrons of Lorentz factor γ injected in the source at the rate of Q electrons per second produce the observed flux at the peak of the synchrotron and SSC components. With five model parameters and five observables, namely the peak frequency of the synchrotron component ν_s , the peak frequency of the SSC component ν_{SSC} , the peak luminosity of the synchrotron component L_s , the Compton dominance k (the ratio of the GeV to synchrotron luminosity), and the variability timescale t_{var} of the gamma ray emission, the system of equations is closed and the Doppler factor of the emission region is given by the following expression that contains only observables:

$$\delta = 100 \left[\frac{2}{c^3 B_{cr}^2} \frac{L_{s,46} \nu_{ssc,22}^2}{\nu_{s,13}^4 t_{var,1d}^2 k_2} \right]^{1/4} \quad (13)$$

where $B_{cr} = 4.4 \times 10^{13}$ G is the critical magnetic field, $\nu_{s,13} = \nu_s/10^{13}\text{Hz}$, $\nu_{ssc,22} = \nu_{SSC}/10^{22}\text{Hz}$, $L_{s,46} = L_s/10^{46}\text{erg s}^{-1}$, $k_2 = k/100$ and $t_{var,1d}$ is the variability timescale of the gamma ray emission region in units of one day, all typical values for powerful blazars (e.g. [Abdo et al. 2010](#); [Bonnoli et al. 2011](#)). For the powerful blazars, on which we focus here, the Doppler factor given by equation (13) is significantly higher than the typical values found from superluminal proper-motions studies (e.g. [Lister et al. 2009](#); [Jorstad et al. 2001](#)). In addition, such high δ values require either a jet with an opening angle of $\sim 1/\delta$ that is extremely well aligned to the observer and therefore with unrealistic de-projected lengths, or a jet with opening angle much greater than $1/\delta$ that would have to be extremely powerful. For these reasons, we disfavor a SSC interpretation of the GeV emission of powerful blazars. Similar conclusions about the inadequacy of the SSC process for powerful blazars have been reached before (e.g., [Abdo et al. 2010](#)).

The SSC process can still be important for powerful blazars, as the synchrotron photon energy density in the spine comoving frame $U_s = L_{s,46}/(4\pi c^3 t_{var}^2 \delta^6)$ can be a non-negligible fraction of the photon energy U'' in the spine due to the sheath radiation reprocessed by the clouds. For reasonable jet parameters, the peak of the SSC SED is in the hard X-ray regime. For example, using equation (13) with $\delta = 10$ and requiring that the SSC component has comparable power to the synchrotron one ($k = 1$), we find that the peak of the SSC component is at $\nu_{SSC} = 10^{19}$ Hz, an energy of ~ 40 KeV. This is in agreement with modeling of the SEDs of powerful blazars (e.g., [Böttcher et al. 2013](#)).

3. AN EXAMPLE SED

We now apply the above scenario to evaluate if the resulting SED from the spine compares well to that of high-power blazars. The SED of powerful blazars is characterised by two spectral components, the first peaking at sub-mm to IR and the second below/around ~ 100 MeV, with the high energy component dominating in apparent luminosity by $\sim 10 - 100$. In the context of leptonic models there is significant contribution or even dominance of SSC at the X-ray band (e.g., [Sikora et al. 1994](#)).

To simulate our proposed scenario we adopt a covering factor $C = 0.1$, a sheath plasma Lorentz factor $\Gamma_{sh} = 3$ and a ratio $a = R_{out}/R_{sh} = 3$. With this set of parameters, using equation (12) we find that the energy density in the spine's rest frame due to the MT is a factor of 10 higher than the energy density of the radiation coming directly from the sheath. We then use the above parameters

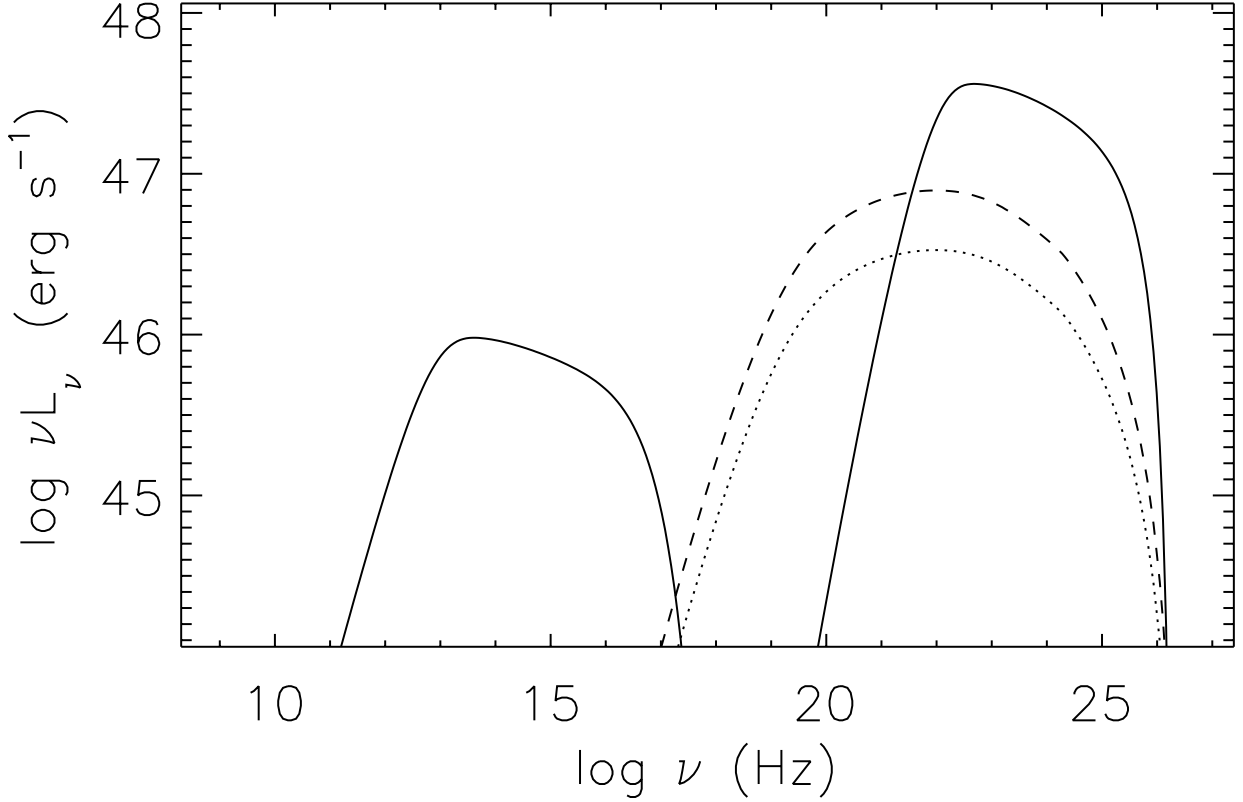


Figure 2. The SED resulting from the parameter values motivated in §3. The low frequency solid line is the spine synchrotron SED, while the high frequency solid line is the spine IC emission from seed photons coming from the MT that is heated by the sheath emission. The broken line is due to SSC within the spine. We also anticipate spine IC emission with the seed photons being sheath synchrotron photons directly entering the spine. As discussed, for this component we anticipate a level of ~ 10 below the IC component resulting from seed photons coming from the MT, but its exact spectral shape depends on the unobservable synchrotron emission of the sheath. For demonstration purposes, we plot this component as a dotted line, assuming an SED similar to the spine’s SSC component but with a peak luminosity ~ 10 times lower than the spine IC emission resulting from the MT seed photons.

in equation (9) to find $U'' = 1.2 \times 10^{-2} \text{ erg cm}^{-3}$ by setting $T_{sub} = 1200 \text{ K}$, $\eta = L_{sh,obs}/L_* = 1/2$, and $\Gamma_{sp} = 20$ (note that at distances of several pc the energy density of the accretion disk and BLR are at least $\sim \Gamma_{sp}^4$ lower as their photons are entering the spine from behind). To obtain a Compton dominance of ~ 30 , we require $B = (U''/(30 \times 8\pi))^{1/2} = 0.1 \text{ G}$.

The spectrum of the reprocessed by the MT radiation of the sheath will be a superposition of black bodies with the hottest coming from the innermost radius R_{sh} and the coolest coming from the outermost radius of the MT R_{out} , with $T(r) = (L_{sh,obs}/16\pi\sigma r^2)^{1/4}$. Using this and equation (3) we obtain $T(R_{sh}) = \eta^{1/4}T_{sub}$ and $T(R_{out}) = a^{-1/2}\eta^{1/4}T_{sub}$. This means that for small values of a , as in this example where $a = 3$, the temperature ratio $T(R_{sh})/T(R_{out}) = a^{1/2}$, is not a large number and we can approximate the SED of the sheath radiation with a single black body function at $T_{eff} = [T(R_{sh})T(R_{out})]^{1/2}$ and energy density in the spine rest frame given by equation (9), which can now be written as

$$U'' = \frac{4\sigma T_{eff}^4}{c} \frac{C \Gamma_{sp}^2}{\Gamma_{sh}^2}, \quad (14)$$

an expression that absorbs η and a in the definition of T_{eff} .

To reproduce typical variability timescales of a few hours to a day, we set the spine radius $R_{sp} = 2 \times 10^{16}$ cm. The electron energy distribution (EED) injected in the spine is a power law of index $p = 2.5$ confined between electron Lorentz factors γ_{min} and γ_{max} . Because the system is in the fast cooling regime, the peaks of the synchrotron and IC emission are produced by electrons of Lorentz factor $\sim \gamma_{min}$. Requiring a synchrotron peak at $\nu_s \approx 10^{13}$ Hz, sets $\gamma_{min} = 10^3$. The requirement that the synchrotron mechanism cuts off before the X-rays is satisfied with $\gamma_{max} = 10^5$. The comoving injected power is set by requiring a blazar GeV luminosity of $L_{GeV} \approx 5 \times 10^{47}$ erg s $^{-1}$, as seen in bright GeV blazars (e.g. [Abdo et al. 2010](#)). Using an equation similar to equation (1), we find $L_{inj} = L_{GeV}/(4\Gamma_{sp}^3) = 2 \times 10^{43}$ erg s $^{-1}$. Using the parameter values we just motivated, we plot in figure (2) the SED produced by the spine. Our single-zone code applies an implicit numerical scheme for solving the electron kinetic equation similar to that of [Graff et al. \(2008\)](#), first introduced by [Chang & Cooper \(1970\)](#). Our code follows the radiative losses in the injected EED and uses the full Klein-Nishina cross section for IC scattering energy losses and emission calculations.

4. CONCLUSIONS AND DISCUSSION

Recent mutiwavelength campaigns (e.g. [Marscher et al. 2010](#)) strongly suggest that a fraction of the *Fermi* observed blazar flares take place a few to several pc from the central engine. At these distances there is no significant external photon field for producing the GeV emission of observed blazar gamma-ray flares via IC scattering from jet relativistic electrons: the BLR is confined within the IR-bright inner part of the MT, which in turn does not exceed a distance of ~ 1 pc from the central engine (e.g. [Koshida et al. 2014](#); [Nenkova et al. 2008](#)) for the powerful sources under consideration. A plausible solution is a spine-sheath geometry for the emitting region ([MacDonald et al. \(2015\)](#)), but see [Nalewajko et al. \(2014\)](#) that argue that this mechanism would become relevant only for observed sheath luminosity that would rival that of the spine).

Here we suggest another seed photon mechanism. We start by adopting a picture of the MT that extends for a few pc beyond the IR-emitting inner radius and has a dust cloud angular distribution that extends with a diminishing density to small polar angles (e.g., [Nenkova et al. 2008](#)).

We then show that for a spine-sheath jet configuration located within the MT there is a reasonable part of parameter space in which the seed photon energy density in the spine is dominated by sheath photons that have been reprocessed by the dust clouds within the wide opening angle of the sheath synchrotron radiation. This differs from the model of [Ghisellini & Madau \(1996\)](#), as it avoids the problem of requiring reprocessing clouds to be within the very small opening angle of the spine radiation.

We explore now plausible values of the AGN covering factor at low polar angles. Recent high resolution mid-IR observations and modeling of nearby quasars ([Martínez-Paredes et al. 2017](#)) with the clumpy molecular torus model ([Nenkova et al. 2008](#)), show that non-negligible covering factors are plausible at small polar angles: for a cloud distribution $N = N_0 \text{Exp}[-(\theta - 90^\circ)^2/\sigma^2]$, where N_0 is the number of clouds encountered by a line of sight in the equatorial direction, σ is the $1/e$ angular opening of the clumpy torus and θ is the angle of the line of sight to the polar direction, the covering factor of the clouds at θ is $C = 1 - e^{-N}$. Adopting $N_0 = 5$, $\sigma = 30^\circ$, $\theta = 30^\circ$, within a wide permitted range (see table 11 of [Martínez-Paredes et al. 2017](#)), we obtain a covering factor of 0.1. This shows that a clumpy molecular torus can provide a non-negligible covering factor at low polar angles.

Variability in our model can result from a range of disturbances in the system. We consider here two types of variations in the injected EED. In the first case the injected EED amplitude increase takes place only in the sheath. Then, for both the spine-sheath-only model and the spine-sheath embedded in the MT model the synchrotron emission of the spine is not expected to vary significantly, as neither the spine magnetic field, nor the spine EED varies. This would result in GeV orphan flares as in blazar PKS 1222+216 (Ackermann et al. 2014). A difference between the two models that could be used to discriminate between them, is that while in the spine-sheath embedded in the MT model only the GeV part of the high energy component should vary, in the spine-sheath only model the hard X-ray to MeV flux would also vary with similar amplitude. This is because the MT-embedded spine-sheath model (spine-sheath only model) seed photons have a narrow (broad) spectral distribution, and this is reflected in the energy width of their IC spectra. Consider now the case where in the MT-embedded spine-sheath model the maximum energy of the EED increases in both the spine and the sheath. In this case the luminosity of both the spine and the sheath increases and it is possible that dust is sublimated within the sheath radiation opening angle (that would be the case when $L_{sh,obs} > L_*$). If the maximum EED energy increases sufficiently, the synchrotron production of UV ionizing photons will illuminate the clouds from which the dust has been sublimated, which in turn will produce line emission (we think of such clouds as parts of the polar part of the MT, possibly parts of an outflow, e.g., Netzer 2015). This line emission would temporally correlate with the optical-UV variations of the spine and sheath synchrotron emission. Such correlations between the optical-UV continuum and emission line variability has been tentatively detected by Isler et al. (2013) and León-Tavares et al. (2013) in the blazar 3C 454.3 and very recently reported with high statistical significance by Jorstad et al. (2017) in the blazar CTA 102.

MG acknowledges support from Fermi grant NNX14AQ71G

REFERENCES

- Abdo, A. A., Ackermann, M., Ajello, M., et al. 2010, *ApJ*, 722, 520
- Ackermann, M., Ajello, M., Allafort, A., et al. 2014, *ApJ*, 786, 157
- Antonucci, R. 1993, *ARA&A*, 31, 473
- Blandford, R. D., & Rees, M. J. 1978, *BL Lac Objects*, 328
- Błażejowski, M., Sikora, M., Moderski, R., & Madejski, G. M. 2000, *ApJ*, 545, 107
- Böttcher, M., Reimer, A., Sweeney, K., & Prakash, A. 2013, *ApJ*, 768, 54
- Bonnoli, G., Ghisellini, G., Foschini, L., Tavecchio, F., & Ghirlanda, G. 2011, *MNRAS*, 410, 368
- Chang, J. S., & Cooper, G. 1970, *Journal of Computational Physics*, 6, 1
- Dermer, C. D., Schlickeiser, R., & Mastichiadis, A. 1992, *A&A*, 256, L27
- Dermer, C. D., & Schlickeiser, R. 1994, *ApJS*, 90, 945
- Elitzur, M. 2012, *ApJL*, 747, L33
- Fuller, L., Lopez-Rodriguez, E., Packham, C., et al. 2016, *MNRAS*, 462, 2618
- Gallimore, J. F., Elitzur, M., Maiolino, R., et al. 2016, *ApJL*, 829, L7
- García-Burillo, S., Combes, F., Ramos Almeida, C., et al. 2016, *ApJL*, 823, L12
- García-González, J., Alonso-Herrero, A., Hönig, S. F., et al. 2017, *MNRAS*, 470, 2578
- Graff, P. B., Georganopoulos, M., Perlman, E. S., & Kazanas, D. 2008, *ApJ*, 689, 68-78
- Ghisellini, G., Tavecchio, F., & Chiaberge, M. 2005, *A&A*, 432, 401
- Ghisellini, G., & Madau, P. 1996, *MNRAS*, 280, 67
- Hada, K., Doi, A., Kino, M., et al. 2011, *Nature*, 477, 185
- Isler, J. C., Urry, C. M., Coppi, P., et al. 2013, *ApJ*, 779, 100

- Jorstad, S. G., Marscher, A. P., Mattox, J. R., et al. 2001, *ApJS*, 134, 181
- Jorstad, S. G., Marscher, A. P., Williamson, K. E., et al. 2017, *AAS/High Energy Astrophysics Division*, 16, 106.02
- Kishimoto, M., Hönic, S. F., Antonucci, R., et al. 2011, *A&A*, 527, A121
- Koshida, S., Minezaki, T., Yoshii, Y., et al. 2014, *ApJ*, 788, 159
- Khim, H., & Yi, S. K. 2017, *ApJ*, in press
- Krolik, J. H., & Begelman, M. C. 1988, *ApJ*, 329, 702
- León-Tavares, J., Chavushyan, V., Patiño-Álvarez, V., et al. 2013, *ApJL*, 763, L36
- Lister, M. L., Cohen, M. H., Homan, D. C., et al. 2009, *AJ*, 138, 1874
- MacDonald, N. R., Marscher, A. P., Jorstad, S. G., & Joshi, M. 2015, *ApJ*, 804, 111
- Maraschi et al., 1992, *ApJ*, 397: L5-L9
- Martínez-Paredes, M., Aretxaga, I., Alonso-Herrero, A., et al. 2017, *MNRAS*, 468, 2
- Marscher, A. P., Jorstad, S. G., Larionov, V. M., et al. 2010, *ApJL*, 710, L126
- Meyer, E. T., Fossati, G., Georganopoulos, M., & Lister, M. L. 2011, *ApJ*, 740, 98
- Nalewajko, K., Begelman, M. C., & Sikora, M. 2014, *ApJ*, 789, 161
- Nenkova, M., Sirocky, M. M., Nikutta, R., Ivezić, Ž., & Elitzur, M. 2008, *ApJ*, 685, 160-180
- Netzer, H. 2015, *ARA&A*, 53, 365
- Sikora, M., Begelman, M. C., & Rees, M. J. 1994, *ApJ*, 421, 153